CHAPTER 6

Projection on Conceptual Design of an Absorption Heat Transformer Coupling with a Vapor Compression Heat Pump

In this chapter, projection of a conceptual design of the 10 kW_{th} compression/absorption heat transformer (CAHT) performance in the previous chapter to a bigger scale of a CAHT is presented. Projection of the absorption heat transformer (AHT) scale is in a range of 10-350 kW_{th}.

6.1 Introduction

Absorption heat transformer (AHT) has been used to recover waste heat which could be upgraded and used in a higher temperature application. However, the system COP is not high due to a high heat loss at the system condenser. To solve this problem, Chaiyat and Kiatsiriroat (2010) has proposed a technique by integrating a vapor compression heat pump (VCHP) to recover the heat rejected at the AHT condenser and transfer it back to the AHT evaporator. It could be found that the overall COP of the whole system which is called the compression/absorption heat transformer (CAHT) could be improved.

In this chapter, performance analysis of a CAHT is carried out when its input parameters such as temperature and flow rate of hot water are prescribed. The projection of the heating capacity of the CAHT could be estimated.

6.2 Projection of the CAHT System by Using Performance Curve of the 10 kW_{th} CAHT

A set of performance curves in Chapter 4 of the 10 kW_{th} CAHT is used to project a trend to improve the thermal performance of the AHT system by combining with the VCHP. Figure 6.1 shows a schematic diagram of a CAHT used for the calculation. The output heat rate at the AHT absorber is in a range of 10-350 kW_{th} by supplying hot water temperature between 50- 95 $^{\circ}C$ at the AHT generator. LiBr-water

is the working pair in the AHT cycle while R-134A and R-123 are the working fluids in the VHP cycles.

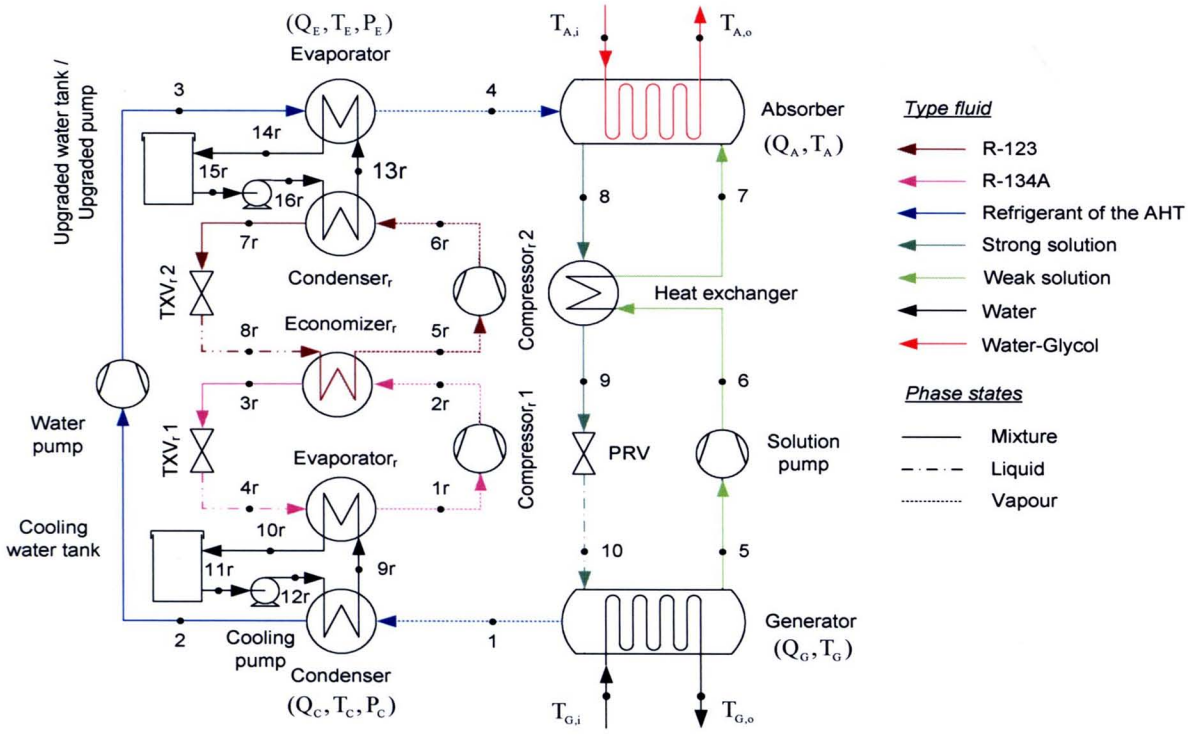

Figure 6.1 The schematic diagram of the compression/absorption heat transformer (CAHT) system.

Figure 6.2 shows the steps for calculating the system performance. The performance correlations of the VCHP system and the AHT system in Chapter 4 are used to predict thermal performance as shown in equations 6.1 and 6.2. The main objective of this simulation is to study the effects of hot water temperature and mass flow rate entering the CAHT on heating capacity at the AHT absorber (Q_A), electrical power consumption of the CAHT (W_{VCHP} and W_{AHT}) and upgraded temperature heat leaving the AHT absorber ($T_{A,o}$). The results are presented as a set of performance curves.

For the VCHP system:

$$EER_{VCHP} = -0.037(T_{HW,i} - T_{CW,i}) + 4.4715, (kW_{th}/kW_e). \quad (6.1)$$

For the AHT system:

$$EER_{AHT} = -10.463(T_{A,i}-T_E)/(T_{G,i}-T_C) + 7.5228. \quad (6.2)$$

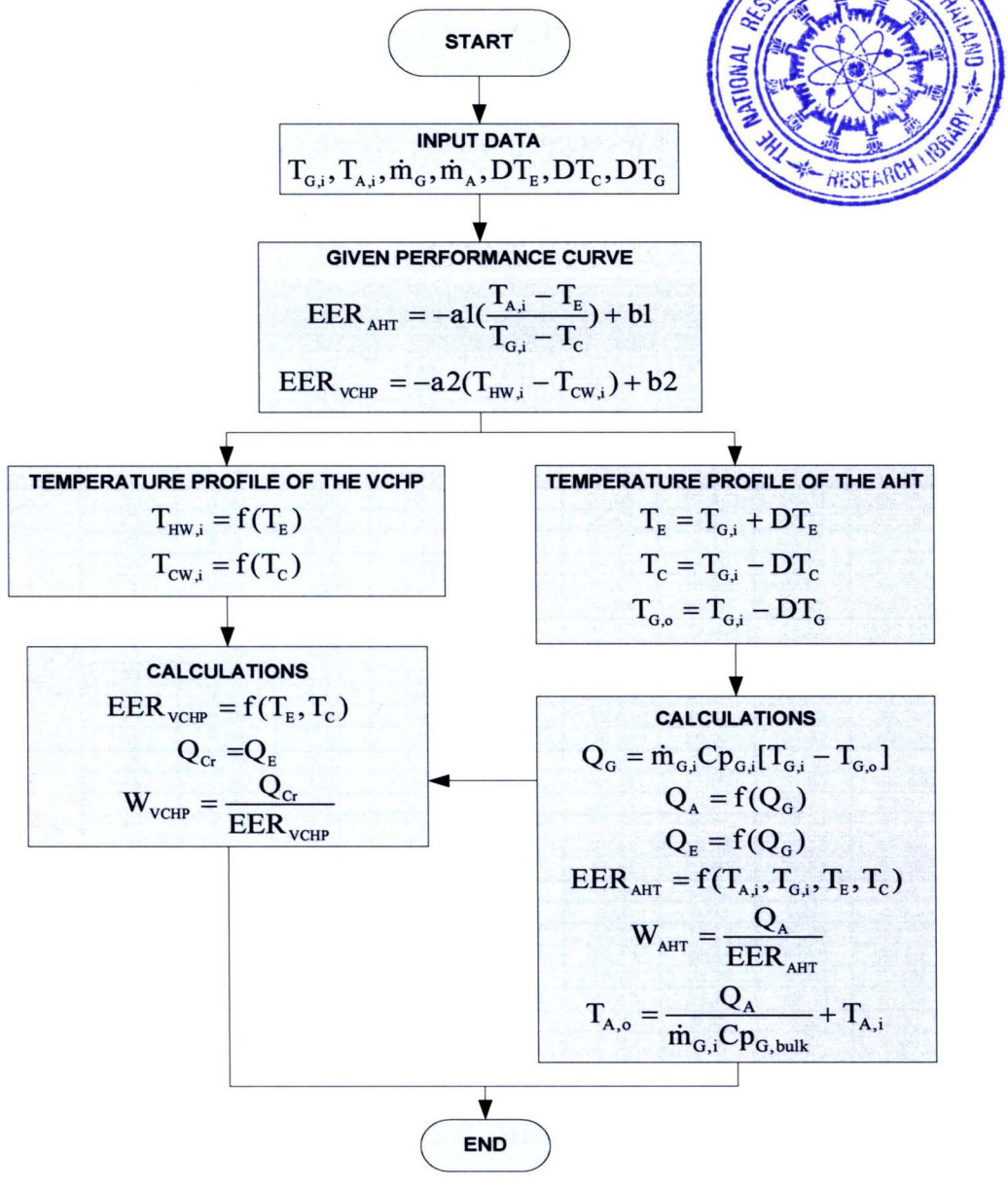

Figure 6.2 The steps for calculating the projection of the CAHT system by using performance curve of the 10 kW_{th} CAHT at upgrading hot water temperature around 90-110 °C.

6.3 Results

From the simplified models as described in Chapter 4, the input parameters which are hot water temperature entering the AHT generator and the AHT absorber ($T_{G,i}$ and $T_{A,i}$), the AHT condenser temperature (T_C), the AHT evaporator temperature

(T_E) and flow rate of hot water entering the CAHT system ($\dot{m}_{G,i}$) are prescribed then the electrical power consumptions of the AHT system (W_{AHT}) and the VCHP system (W_{VCHP}) are evaluated. The results are shown in Table 6.1 and Table 6.2, respectively.

Table 6.1 The prediction of the electrical power consumption of the AHT system.

$T_{G,i} = T_{A,i}$	T_C	T_E	EER_{AHT}	W_{AHT} (kW$_e$)							
				$m_{G,i} = 0.5$	$m_{G,i} = 1.5$	$m_{G,i} = 3$	$m_{G,i} = 5$	$m_{G,i} = 8$	$m_{G,i} = 10$	$m_{G,i} = 12$	$m_{G,i} = 15$
				A	B	C	D	E	F	G	H
50	0	35	4.38	2.38	7.15	14.31	23.85	38.15	47.69	57.23	71.54
60		45	4.91	2.13	6.40	12.79	21.32	34.12	42.64	51.17	63.97
70		55	5.28	1.98	5.95	11.90	19.84	31.74	39.67	47.61	59.51
80		65	5.56	1.89	5.66	11.32	18.87	30.19	37.73	45.28	56.60
90		75	5.78	1.82	5.46	10.92	18.19	29.11	36.38	43.66	54.58
100		85	5.95	1.77	5.31	10.62	17.70	28.32	35.41	42.49	53.11
50	10	35	3.60	2.90	8.71	17.43	29.05	46.47	58.09	69.71	87.14
60		45	4.38	2.39	7.16	14.32	23.87	38.19	47.73	57.28	71.60
70		55	4.91	2.13	6.40	12.81	21.35	34.16	42.70	51.24	64.04
80		65	5.28	1.99	5.96	11.92	19.87	31.79	39.74	47.69	59.61
90		75	5.56	1.89	5.67	11.34	18.91	30.25	37.81	45.37	56.72
100		85	5.78	1.82	5.47	10.94	18.24	29.18	36.47	43.77	54.71
50	20	35	2.29	4.56	13.69	27.37	45.62	73.00	91.25	109.50	136.87
60		45	3.60	2.91	8.72	17.44	29.07	46.51	58.14	69.77	87.21
70		55	4.38	2.39	7.17	14.34	23.90	38.23	47.79	57.35	71.69
80		65	4.91	2.14	6.41	12.83	21.38	34.21	42.76	51.32	64.15
90		75	5.28	1.99	5.97	11.95	19.91	31.85	39.82	47.78	59.73
100		85	5.56	1.90	5.69	11.37	18.95	30.32	37.90	45.48	56.86
50	30	35	0.00	0.00	0.00	0.00	0.00	0.00	0.00	0.00	0.00
60		45	2.29	4.57	13.70	27.40	45.66	73.06	91.33	109.59	136.99
70		55	3.60	2.91	8.73	17.46	29.11	46.57	58.21	69.85	87.32
80		65	4.38	2.39	7.18	14.36	23.93	38.29	47.87	57.44	71.80
90		75	4.91	2.14	6.43	12.85	21.42	34.28	42.85	51.42	64.27
100		85	5.28	2.00	5.99	11.97	19.96	31.93	39.92	47.90	59.87
50	40	35	0.00	0.00	0.00	0.00	0.00	0.00	0.00	0.00	0.00
60		45	0.00	0.00	0.00	0.00	0.00	0.00	0.00	0.00	0.00
70		55	2.29	4.57	13.72	27.43	45.72	73.15	91.44	109.73	137.16
80		65	3.60	2.92	8.75	17.49	29.15	46.64	58.30	69.96	87.45
90		75	4.38	2.40	7.19	14.39	23.98	38.37	47.96	57.56	71.94
100		85	4.91	2.15	6.44	12.89	21.48	34.36	42.96	51.55	64.43
50	50	35	0.00	0.00	0.00	0.00	0.00	0.00	0.00	0.00	0.00
60		45	0.00	0.00	0.00	0.00	0.00	0.00	0.00	0.00	0.00
70		55	0.00	0.00	0.00	0.00	0.00	0.00	0.00	0.00	0.00
80		65	2.29	4.58	13.74	27.47	45.79	73.27	91.58	109.90	137.37
90		75	3.60	2.92	8.76	17.53	29.21	46.74	58.42	70.10	87.63
100		85	4.38	2.40	7.21	14.42	24.04	38.47	48.08	57.70	72.12

The results from Table 6.1 could be performed a set of graphs those show the relations among $T_{G,i}$, T_C, T_E and $\dot{m}_{G,i}$ on W_{AHT} as shown in Figure 6.3 and Figure 6.4.

By giving the entering water temperature at the generator of the CAHT ($T_{G,i}$) as state ① and the value is assumed to equal the water temperature entering the AHT absorber ($T_{A,i}$) and with selected T_C and T_E of the absorption cycle at state ②, the energy efficiency ratio (EER_{AHT}) is the output as shown at state ③. Then, EER_{AHT} is used to find out the W_{AHT} of the absorption system in Figure 6.4 and the outputs

which are $\dot{m}_{G,i}$ and W_{AHT} could be taken at state ④ and state ⑤, respectively. For the VCHP, W_{VCHP} could be estimated form Table 6.2 by using W_{AHT} in Table 6.1 which shows the corrosion in term of symbol A-H.

Table 6.2 The prediction of the electrical power consumption of the VCHP system.

$T_{G,i} = T_{A,i}$	T_C	T_E	EER_{VCHP}	W_{VCHP} (kW_e)							
				$m_{G,i} = 0.5$	$m_{G,i} = 1.5$	$m_{G,i} = 3$	$m_{G,i} = 5$	$m_{G,i} = 8$	$m_{G,i} = 10$	$m_{G,i} = 12$	$m_{G,i} = 15$
				A	B	C	D	E	F	G	H
50	0	35	3.18	3.62	10.86	21.72	36.20	57.92	72.40	86.88	108.60
60		45	2.81	4.10	12.29	24.58	40.97	65.56	81.95	98.34	122.92
70		55	0.00	0.00	0.00	0.00	0.00	0.00	0.00	0.00	0.00
80		65	0.00	0.00	0.00	0.00	0.00	0.00	0.00	0.00	0.00
90		75	0.00	0.00	0.00	0.00	0.00	0.00	0.00	0.00	0.00
100		85	0.00	0.00	0.00	0.00	0.00	0.00	0.00	0.00	0.00
50	10	35	3.55	3.24	9.73	19.45	32.42	51.88	64.85	77.82	97.27
60		45	3.18	3.62	10.87	21.74	36.23	57.97	72.46	86.96	108.70
70		55	2.81	4.11	12.32	24.64	41.06	65.69	82.12	98.54	123.18
80		65	2.44	4.74	14.21	28.42	47.37	75.79	94.74	113.69	142.11
90		75	2.07	3.26	0.00	0.00	0.00	0.00	0.00	0.00	0.00
100		85	1.70	4.33	0.00	0.00	0.00	0.00	0.00	0.00	0.00
50	20	35	3.92	2.94	8.81	17.62	29.36	46.98	58.72	70.47	88.08
60		45	3.55	3.25	9.74	19.47	32.45	51.92	64.90	77.88	97.36
70		55	3.18	3.63	10.88	21.77	36.28	58.04	72.55	87.06	108.83
80		65	2.81	4.11	12.34	24.67	41.12	65.80	82.25	98.70	123.37
90		75	2.44	4.75	14.24	28.48	47.46	75.94	94.93	113.91	142.39
100		85	0.00	0.00	0.00	0.00	0.00	0.00	0.00	0.00	0.00
50	30	35	0.00	0.00	0.00	0.00	0.00	0.00	0.00	0.00	0.00
60		45	3.92	2.94	8.82	17.63	29.39	47.02	58.77	70.53	88.16
70		55	3.55	3.25	9.75	19.49	32.49	51.99	64.98	77.98	97.47
80		65	3.18	3.63	10.90	21.80	36.33	58.13	72.67	87.20	109.00
90		75	2.81	4.12	12.36	24.72	41.21	65.93	82.41	98.89	123.62
100		85	2.44	4.76	14.27	28.55	47.58	76.13	95.16	114.19	142.74
50	40	35	0.00	0.00	0.00	0.00	0.00	0.00	0.00	0.00	0.00
60		45	0.00	0.00	0.00	0.00	0.00	0.00	0.00	0.00	0.00
70		55	3.92	2.94	8.83	17.65	29.42	47.08	58.84	70.61	88.27
80		65	3.55	3.25	9.76	19.53	32.54	52.07	65.09	78.10	97.63
90		75	3.18	3.64	10.92	21.84	36.41	58.25	72.81	87.38	109.22
100		85	2.81	4.13	12.39	24.78	41.31	66.09	82.62	99.14	123.92
50	50	35	0.00	0.00	0.00	0.00	0.00	0.00	0.00	0.00	0.00
60		45	0.00	0.00	0.00	0.00	0.00	0.00	0.00	0.00	0.00
70		55	0.00	0.00	0.00	0.00	0.00	0.00	0.00	0.00	0.00
80		65	3.92	2.95	8.84	17.68	29.47	47.15	58.94	70.72	88.41
90		75	3.55	3.26	9.78	19.56	32.61	52.17	65.22	78.26	97.82
100		85	3.18	3.65	10.95	21.90	36.50	58.39	72.99	87.59	109.49

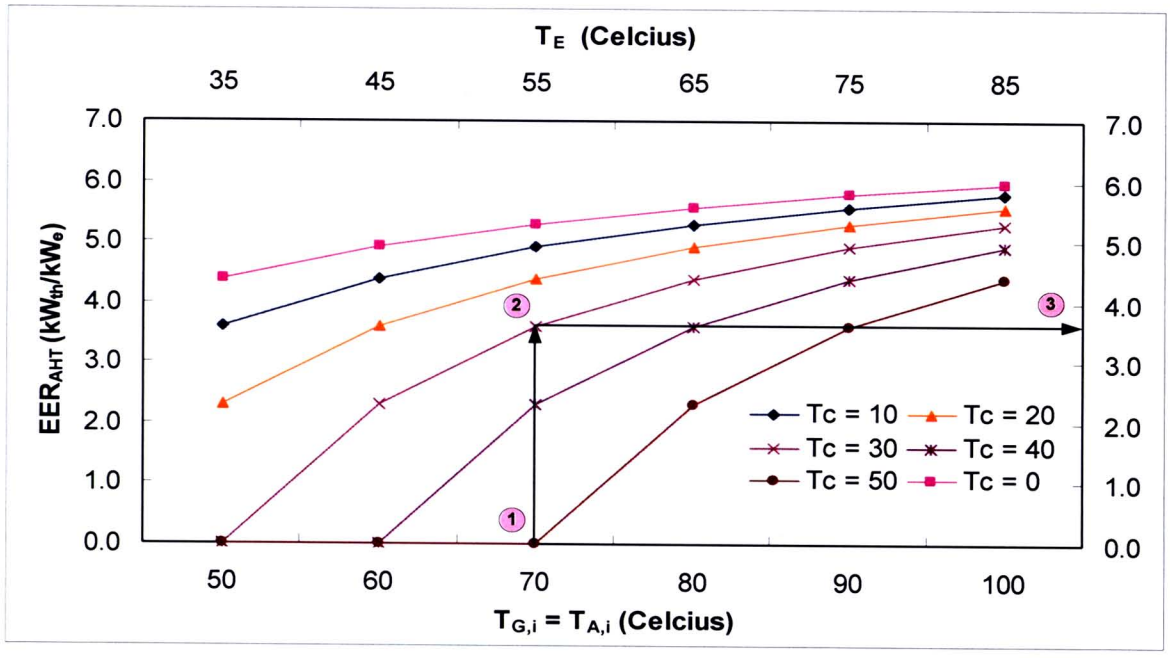

Figure 6.3 The prediction of effect of the $T_{G,i}$, T_C and T_E on the EER_{AHT}.

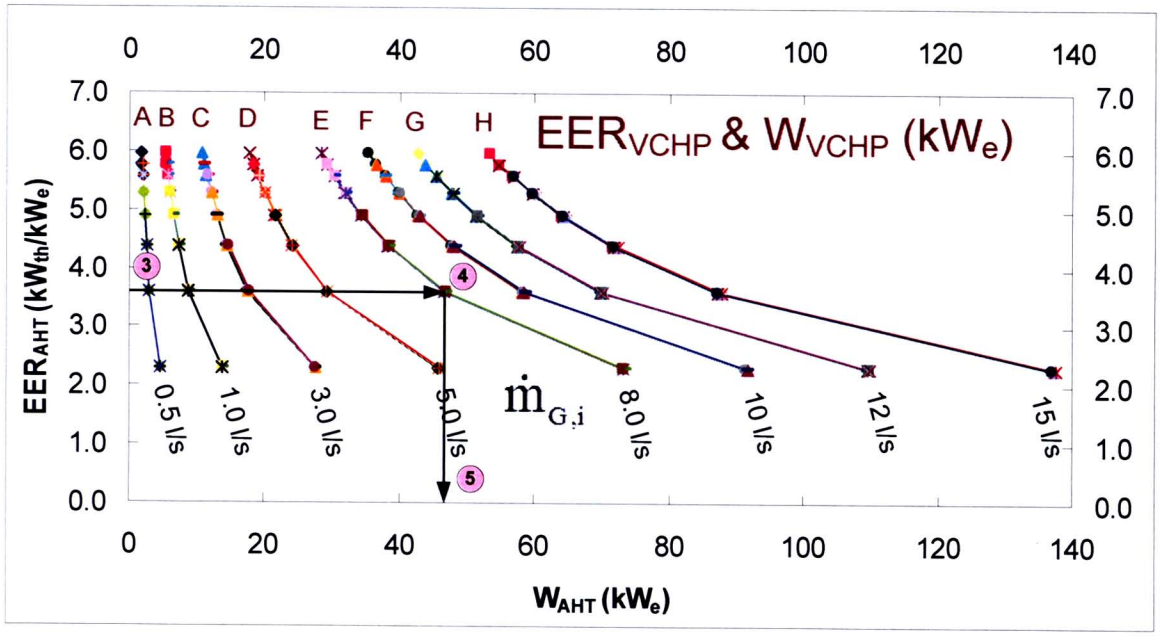

Figure 6.4 The prediction of the EER_{AHT} and W_{AHT}.

Table 6.3 and Table 6.4 show the calculated heating capacity at the AHT absorber (Q_A), the upgraded temperature leaving the CAHT system ($T_{A,o}$) at various values of $T_{G,i}$, T_C and T_E. The correlations of these parameters are plotted in Figure 6.5 and Figure 6.6.

W_{AHT} at state ⑤ from Figure 6.4 for a value of $\dot{m}_{G,i}$ at state ⑥, is used to find out Q_A at state ⑦ in Figure 6.5. Then, Q_A is used to estimate $T_{A,o}$ of the CAHT system at a flow rate $(\dot{m}_{G,i})$ at state ⑧ as shown in Figure 6.6. The value of $T_{A,o}$ is shown as state ⑨. The flow rate of the upgraded fluid $(\dot{m}_{A,i})$ of this Figure is at 1 l/s.

Table 6.3 The prediction of heating capacity at the AHT absorber.

T_C	Q_A (kW)							
	$m_{G,i}$ = 0.5	$m_{G,i}$ = 1.5	$m_{G,i}$ = 3	$m_{G,i}$ = 5	$m_{G,i}$ = 8	$m_{G,i}$ = 10	$m_{G,i}$ = 12	$m_{G,i}$ = 15
0	11.02	33.07	66.13	110.22	176.35	220.44	264.52	330.66
	11.00	32.99	65.98	109.96	175.94	219.92	263.91	329.88
	0.00	0.00	0.00	0.00	0.00	0.00	0.00	0.00
	0.00	0.00	0.00	0.00	0.00	0.00	0.00	0.00
	0.00	0.00	0.00	0.00	0.00	0.00	0.00	0.00
	0.00	0.00	0.00	0.00	0.00	0.00	0.00	0.00
10	10.99	32.96	65.91	109.86	175.77	219.71	263.65	329.57
	10.93	32.79	65.58	109.30	174.88	218.60	262.32	327.90
	10.92	32.75	65.49	109.16	174.65	218.31	261.98	327.47
	10.93	32.77	65.55	109.24	174.79	218.48	262.18	327.73
	0.00	0.00	0.00	0.00	0.00	0.00	0.00	0.00
	0.00	0.00	0.00	0.00	0.00	0.00	0.00	0.00
20	11.10	33.30	66.60	111.00	177.60	222.00	266.41	333.01
	10.88	32.64	65.28	108.80	174.09	217.61	261.13	326.41
	10.84	32.53	65.06	108.43	173.48	216.85	260.22	325.28
	10.84	32.52	65.03	108.39	173.42	216.77	260.12	325.15
	10.85	32.56	65.12	108.53	173.64	217.05	260.46	325.58
	0.00	0.00	0.00	0.00	0.00	0.00	0.00	0.00
30	0.00	0.00	0.00	0.00	0.00	0.00	0.00	0.00
	10.98	32.93	65.86	109.76	175.62	219.53	263.44	329.29
	10.78	32.35	64.70	107.83	172.53	215.66	258.80	323.49
	10.76	32.29	64.58	107.63	172.20	215.25	258.30	322.88
	10.77	32.31	64.62	107.69	172.31	215.39	258.46	323.08
	10.79	32.37	64.74	107.91	172.65	215.82	258.98	323.72
40	0.00	0.00	0.00	0.00	0.00	0.00	0.00	0.00
	0.00	0.00	0.00	0.00	0.00	0.00	0.00	0.00
	10.86	32.58	65.16	108.60	173.76	217.19	260.63	325.79
	10.70	32.09	64.17	106.95	171.12	213.90	256.68	320.85
	10.69	32.07	64.15	106.91	171.06	213.83	256.59	320.74
	10.71	32.13	64.26	107.09	171.35	214.18	257.02	321.27
50	0.00	0.00	0.00	0.00	0.00	0.00	0.00	0.00
	0.00	0.00	0.00	0.00	0.00	0.00	0.00	0.00
	0.00	0.00	0.00	0.00	0.00	0.00	0.00	0.00
	10.75	32.25	64.51	107.51	172.02	215.03	258.03	322.54
	10.62	31.85	63.70	106.17	169.87	212.34	254.81	318.51
	10.63	31.89	63.78	106.30	170.07	212.59	255.11	318.89

Table 6.4 The prediction of the upgraded temperature leaving the CAHT system at $m_{A,i} = 1 l/s$.

T_A (Celcius)							
$m_{G,i} = 0.5$	$m_{G,i} = 1.5$	$m_{G,i} = 3$	$m_{G,i} = 5$	$m_{G,i} = 8$	$m_{G,i} = 10$	$m_{G,i} = 12$	$m_{G,i} = 15$
52.64	57.91	65.82	76.36	92.17	102.72	113.26	129.08
62.63	67.88	75.76	86.27	102.04	112.55	123.06	138.82
0.00	0.00	0.00	0.00	0.00	0.00	0.00	0.00
0.00	0.00	0.00	0.00	0.00	0.00	0.00	0.00
0.00	0.00	0.00	0.00	0.00	0.00	0.00	0.00
0.00	0.00	0.00	0.00	0.00	0.00	0.00	0.00
52.63	57.88	65.76	76.27	92.03	102.54	113.05	128.81
62.61	67.84	75.67	86.12	101.79	112.23	122.68	138.35
72.61	77.82	85.63	96.05	111.68	122.10	132.52	148.15
82.60	87.81	95.62	106.03	121.65	132.06	142.47	158.09
0.00	0.00	0.00	0.00	0.00	0.00	0.00	0.00
0.00	0.00	0.00	0.00	0.00	0.00	0.00	0.00
52.65	57.96	65.93	76.55	92.47	103.09	113.71	129.64
62.60	67.80	75.60	86.00	101.60	112.00	122.40	137.99
72.59	77.76	85.53	95.88	111.40	121.75	132.10	147.63
82.58	87.75	95.50	105.83	121.32	131.65	141.98	157.48
92.58	97.74	105.48	115.81	131.29	141.61	151.94	167.42
0.00	0.00	0.00	0.00	0.00	0.00	0.00	0.00
0.00	0.00	0.00	0.00	0.00	0.00	0.00	0.00
62.62	67.87	75.74	86.23	101.96	112.45	122.95	138.68
72.57	77.72	85.44	95.73	111.17	121.47	131.76	147.20
82.55	87.66	95.31	105.52	120.84	131.05	141.26	156.57
92.56	97.68	105.37	115.61	130.98	141.22	151.46	166.83
102.56	107.68	115.36	125.60	140.96	151.19	161.43	176.79
0.00	0.00	0.00	0.00	0.00	0.00	0.00	0.00
0.00	0.00	0.00	0.00	0.00	0.00	0.00	0.00
72.59	77.78	85.55	95.92	111.47	121.83	132.20	147.75
82.55	87.65	95.29	105.48	120.77	130.97	141.16	156.45
92.54	97.63	105.25	115.42	130.68	140.85	151.02	166.27
102.54	107.62	115.24	125.40	140.65	150.81	160.97	176.21
0.00	0.00	0.00	0.00	0.00	0.00	0.00	0.00
0.00	0.00	0.00	0.00	0.00	0.00	0.00	0.00
0.00	0.00	0.00	0.00	0.00	0.00	0.00	0.00
82.56	87.69	95.37	105.62	120.99	131.24	141.48	156.85
92.52	97.57	105.15	115.25	130.40	140.49	150.59	165.74
102.52	107.56	115.13	125.22	140.34	150.43	160.52	175.64

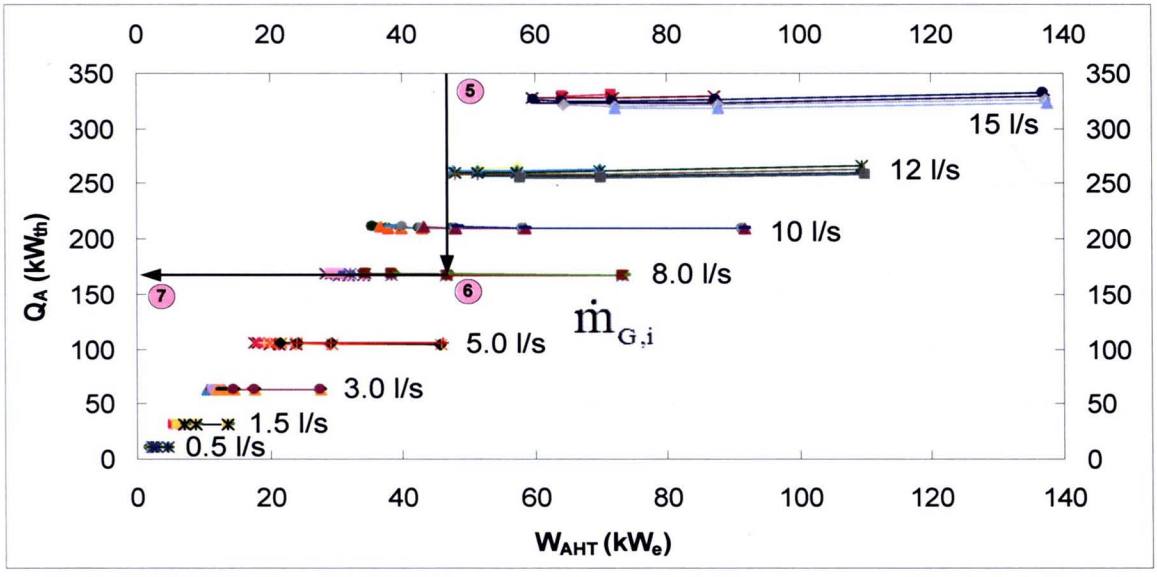

Figure 6.5 The prediction of the energy efficiency of the AHT system in term of W_{AHT} and Q_A at $m_{A,i} = 11/s$.

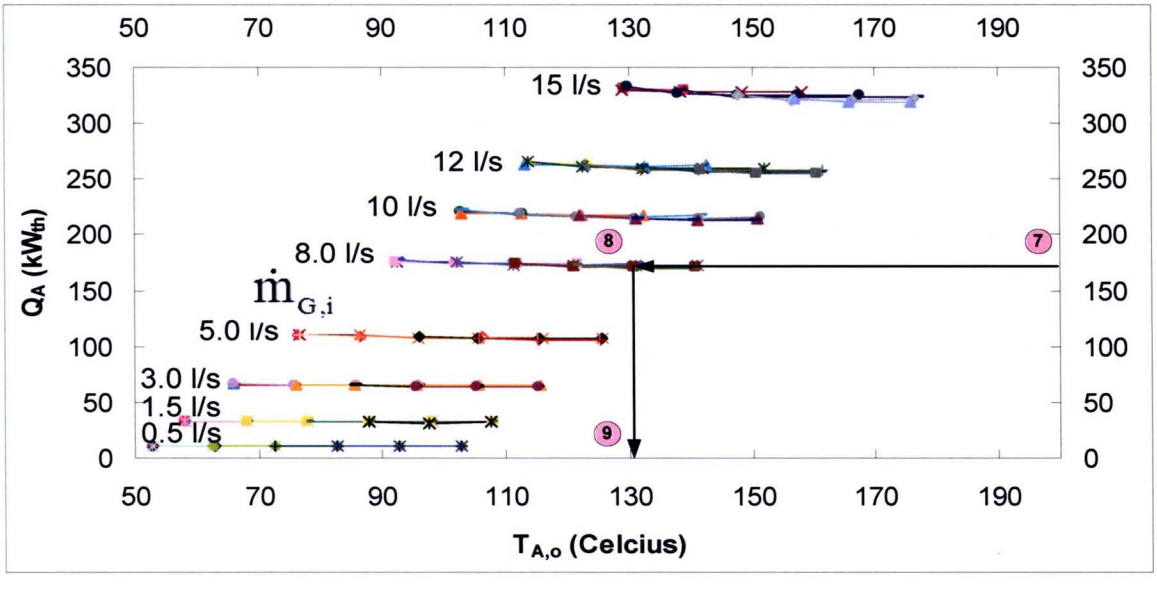

Figure 6.6 The prediction of the upgraded temperature leaving the CAHT ($T_{A,o}$) on Q_A at $m_{A,i} = 11/s$.

The correlations of the CAHT from Figures 6.3-6.6 could be grouping together as shown in Figure 6.7. From the experimental input data in Chapter 4, at hot water temperature 70 °C, AHT condenser 30 °C, AHT evaporator 70 °C and hot water flow rate entering the AHT generator 0.5 l/s, from Figure 6.7, it could be found

that the output temperature and the heat rate at the AHT absorber of the upgraded fluid are around 90 °C and 10 kW, respectively. Figure 6.8 shows the results which agree well with the experimental data in Figures 4.2 and 4.3, respectively. It could be noted that when the mass flow rate of the upgraded fluid, $\dot{m}_{A,i}$, increases, the upgraded temperature $T_{A,o}$ tends to decrease.

6.4 Conclusions

Projection of the heating capacity of the CAHT could be estimated from a set of performance curves developed from the simplified models. The input parameters are hot water temperature entering the AHT generator and the AHT absorber ($T_{G,i}$ and $T_{A,i}$), the AHT condenser temperature (T_C), the AHT evaporator temperature (T_E) and flow rate of hot water entering the CAHT system ($\dot{m}_{G,i}$) then the electrical power consumptions of the AHT system (W_{AHT}) and the VCHP system (W_{VCHP}) could be evaluated. Moreover, the heat rate at the absorber (Q_A) and the upgraded temperature of the working fluid at the absorber ($T_{A,o}$) could be evaluated.

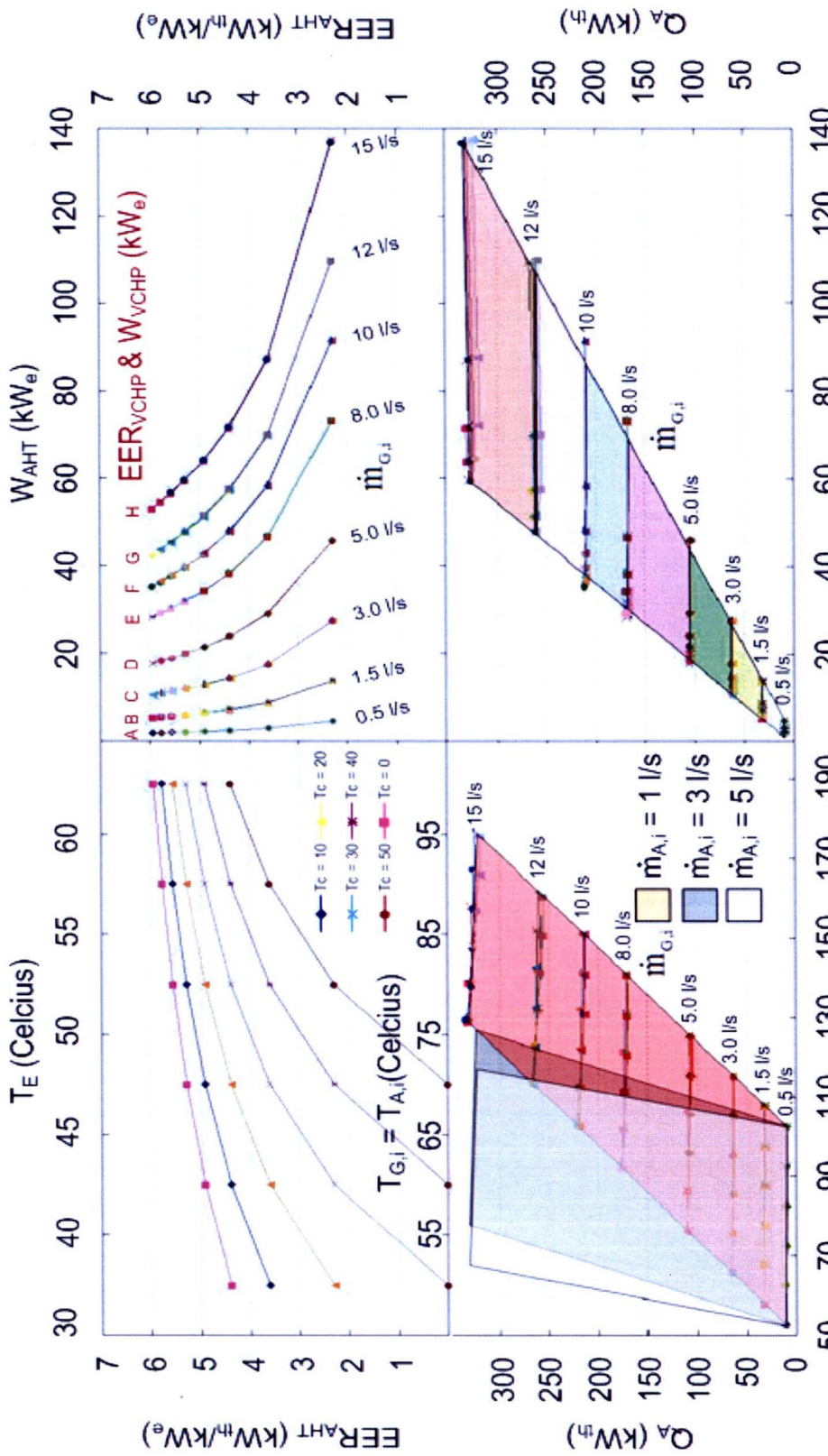

Figure 6.7 The prediction of the thermal performance of the CAHT system.

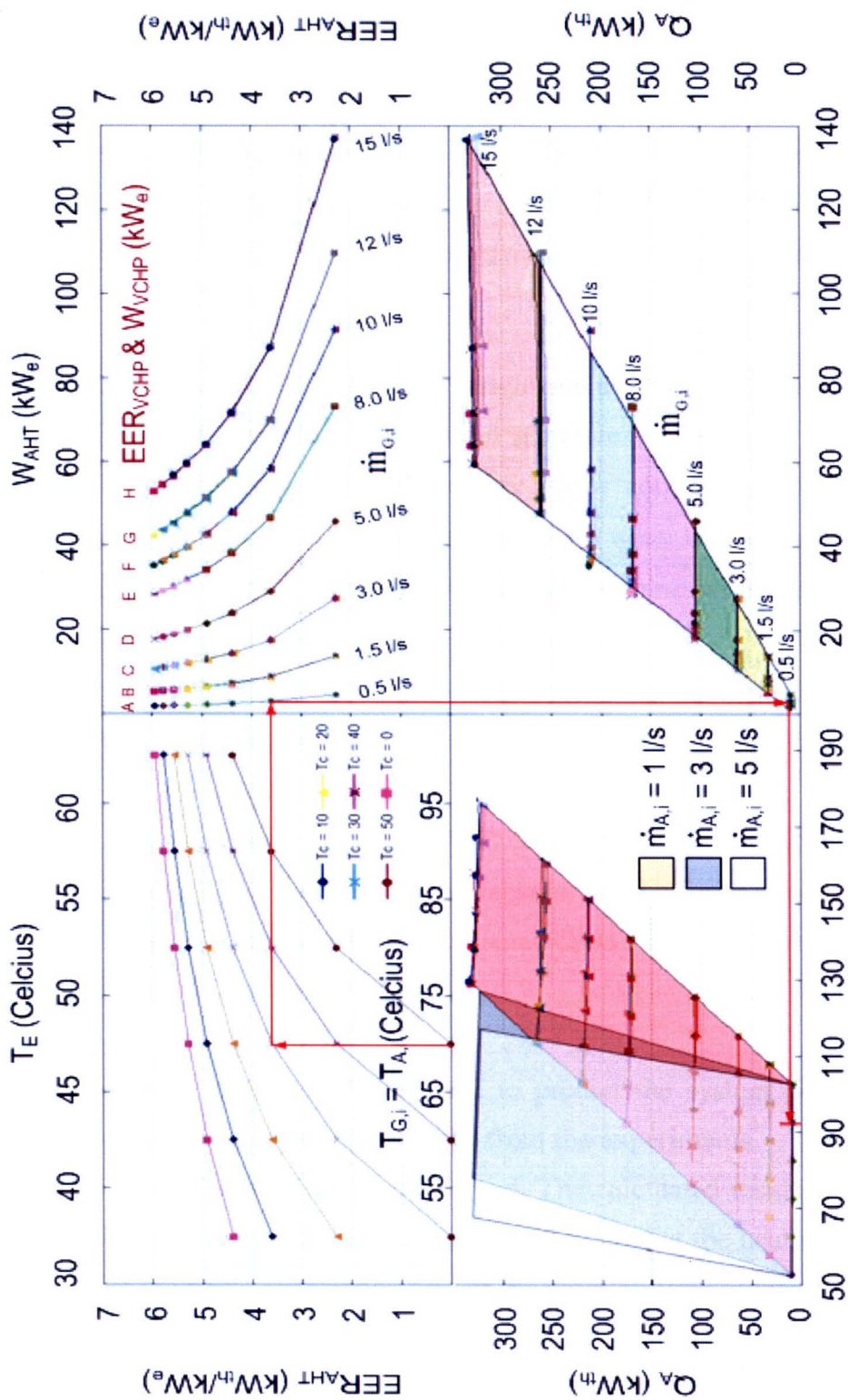

Figure 6.8 Comparison of thermal performance between the experimental data and the results form the CAHT chart performance.